Soil Biology and Biochemistry 203 (2025) 109748

Contents lists available at ScienceDirect

Soil Biology and Biochemistry

journal homepage: www.elsevier.com/locate/soilbio

Bioavailable carbon additions to soil promote free-living nitrogen fixation and microbial biomass growth with N-free lipids

Georg Dittmann [a], Su Ding [b], Ellen C. Hopmans [b], Simon A. Schröter [a], Alice M. Orme [a], Erika Kothe [c], Markus Lange [a], Gerd Gleixner [a,*]

[a] Dept. Biogeochemical Processes, Max Planck Institute for Biogeochemistry, Jena, Germany
[b] Dept. Marine Microbiology & Biogeochemistry, NIOZ Royal Netherlands Institute for Sea Research, Texel, Netherlands
[c] Dept. Microbial Communication, Friedrich-Schiller University, Jena, Germany

ARTICLE INFO

Keywords:
Intact polar lipids (IPL)
Free-living nitrogen fixation (FLNF)
$^{15}N_2$ soil incubation
Microbial energy storage
N-free membrane substitution

ABSTRACT

Globally, the process of atmospheric nitrogen (N_2) fixation by free-living diazotrophs in soils contributes significantly to the soil N supply, yet the understanding of its driving factors, particularly the role of energy availability, is limited. In this study, we explored how two different energy sources, an artificial carbon input, simulating highly bioavailable root exudates, and a natural gradient in soil organic matter that requires decomposition, affect N_2 fixation by free-living diazotrophs and soil microbial community functions through microcosm $^{15}N_2$ incubation experiments. We analysed the incorporation of ^{15}N into soil and used mass spectrometry to determine microbial lipids, which serve as indicators of microbial community functions, via an untargeted lipidomics approach. Our findings demonstrate a significant capacity for N_2 fixation by free-living diazotrophs, with a potential annual storage of 111 kg N per hectare. The addition of artificial exudates yielded an extra of 51 kg N $ha^{-1}y^{-1}$. This N_2 fixation was accompanied by a presumable N limitation in the microbial community, as biomass growth favoured N-free lipids with an equal synthesis of storage (triacylglycerols) and structural membrane lipids. While energy addition boosted N uptake particularly in soils with low organic matter, in soils rich in organic matter, N uptake was naturally higher (an extra 20 kg N $ha^{-1}y^{-1}$), along with increased levels of membrane-associated lipids, suggesting a larger microbial community. Our results imply that enhanced root exudation, potentially driven by more productive plant communities, could mitigate the energy constraints on free-living diazotrophic N_2 fixation as part of a vital soil microbial community. These insights support the development of sustainable agricultural practices that stimulate the capacity for N_2 fixation by free-living diazotrophs, aiming to maintain ecological balance by minimising N loss from fertilisation.

1. Introduction

In many ecosystems, plant productivity is constrained by the availability of nitrogen (N) (Weber and Burow, 2018; Du et al., 2020), a critical nutrient that plants cannot directly access from atmospheric N_2 or decompose from soil organic matter (SOM) (Ashton et al., 2010; Coskun et al., 2017). Instead, they rely on soil microorganisms to symbiotically fix atmospheric N_2 or mineralise SOM, releasing plant-available forms of N such as NH_4^+ and NO_3^- (Krapp, 2015; de Bruijn, 2015; Coskun et al., 2017). Plants actively stimulate the mineralisation by releasing root exudates (Hütsch et al., 2002), which provide energy for SOM decomposition, enhancing microbial activity and growth. However, the energy input into soil microorganisms can lead to nutrient imbalances potentially limiting microbial growth responses (Mason-Jones et al., 2023). To compensate, soil microorganisms have developed strategies such as storing excess energy as lipids (Mason-Jones et al., 2023), fixing atmospheric N_2 via nitrogenase enzymes (Dynarski and Houlton, 2018), and altering their membrane composition from N-containing to N-free lipids (Schubotz, 2019). So far, our understanding of the interplay between the different compensation mechanisms remains limited, and in particular the effects of free-living nitrogen fixation (FLNF) and adaptations in the microbial lipid metabolism are not well considered.

* Corresponding author.
E-mail address: gerd.gleixner@bgc-jena.mpg.de (G. Gleixner).

https://doi.org/10.1016/j.soilbio.2025.109748
Received 26 June 2024; Received in revised form 11 February 2025; Accepted 13 February 2025
Available online 14 February 2025

1.1. Free-living nitrogen fixation

Microbial N_2 fixation is either performed by symbiotic bacteria (e.g., *Rhizobia* and *Frankia* sp.) that live in plant roots or by free-living asymbiotic heterotrophic bacteria (e.g., *Azotobacter* sp.), autotrophic archaea and bacteria (e.g., certain *Cyanobacteria*). The symbiotic fixation of N_2 is a major research line (Poole et al., 2018), whereas the fixation by free-living diazotrophs remains understudied. However, free-living nitrogen fixation (FLNF) occurs worldwide and contributes substantially to the global nitrogen fixation (Dynarski and Houlton, 2018), with estimated average N uptake rates between 1 and 15 kg N $ha^{-1}y^{-1}$ over diverse ecosystems and a range of 0.1–21 kg N $ha^{-1}y^{-1}$ in temperate grasslands (summarised in Reed et al., 2011). $^{15}N_2$ incubation experiments have proven to reproducibly estimate realised and potential N_2 uptake by FLNF (Gupta et al., 2014; Smercina et al., 2019b; Scheibe and Spohn, 2022) with potential uptake rates exceeding the realised ones (Smercina et al., 2019b).

A significant limitation for FLNF are bioavailable carbon (C) sources providing the essential energy for biological N_2 fixation (de Bruijn, 2015). As a result, FLNF predominantly occurs in the rhizosphere, where root exudates provide highly bioavailable C as an energy source (Smercina et al., 2019a), and in hotspots of SOM decomposition (Reed et al., 2011; Zheng et al., 2020). Therefore, increased plant root exudation along with more diverse and productive plant communities (Eisenhauer et al., 2017) may overcome energy constraints on FLNF. However, these exudates also stimulate microorganisms that mineralise SOM (Phillips et al., 2011; Meier et al., 2017), thereby increasing the overall N availability (Lu et al., 2018) and potentially decreasing FLNF. The complex interactions between the plant communities, soil properties and microbial functions, which influence both FLNF and SOM mineralisation remain poorly understood in terms of their impact on nutrient availability and ecosystem functioning. Consequently, it is still uncertain whether FLNF can serve as a sustainable alternative to our current N-fertiliser intensive agriculture (Lassaletta et al., 2014), which exceeds the sustainable planetary boundary for N (Richardson et al., 2023).

1.2. Microbial lipid metabolism

Microbial survival in complex environments depends on adjustable cell membranes composed of diverse structural intact polar lipids (IPL). IPL decay rapidly after cell lysis, making them markers for the living microbial community (White et al., 1979; Sturt et al., 2004). A simultaneous increase of all IPLs indicates cellular growth and operates as a proxy for microbial biomass (Schubotz et al., 2009). In general, IPL can be categorised based on their N or P content (summarised in Sohlenkamp and Geiger, 2016; see also Semeniuk et al., 2014; Hines et al., 2017; Ding et al., 2020). Aminlipids, such as betaine and ornithine lipids (OL), contain N in their structure. Phospholipids either contain both P and N (e.g., phosphatidylethanolamines (PE), phosphatidylcholines (PC)), or only P (e.g., cardiolipins (CL), phosphatidylinositol (PI)). Glycolipids, such as digalactosyl-diacylglycerols (DGDG) are P and N-free. However, the microbial membrane lipid composition is not static. For instance, certain bacteria and fungi, when grown under phosphorus-(P)-limiting conditions, substitute their phospholipids with non-phospholipids such as betaine lipids (Geiger et al., 2010; Riekhof et al., 2014; Warren, 2020; Warren and Butler, 2024), ornithine lipids (Vences-Guzman et al., 2012; Bale et al., 2021) or glycolipids (Bosak et al., 2016) for survival. Comparable adaptations involving glycolipids like DGDG occur in certain phototrophs under N limitation (Abida et al., 2015; Degraeve-Guilbault et al., 2017). The effect of N limitation on the membrane composition of non-phototrophs remains understudied (reviewed in Schubotz, 2019). However, FLNF could overcome N limitation on a community level as it is expected to be more important in low fertile environments with low abundance of symbiotic N-fixers (Reed et al., 2011).

Non-polar lipids, such as C-rich triacylglycerols (TAG) and polyhydroxybutyrate (PHB) play key roles in microbial energy storage (Mason-Jones et al., 2022) and account for considerable portions of the total microbial biomass under both high and low C availability (Mason-Jones et al., 2023). A recent study by Butler et al. (2023) found increased microbial C allocation to neutral lipid fatty acids (NLFA, derived from neutral lipids e.g., TAG) and PHB in infertile soils. In this study, C allocation to PHB was associated primarily with phosphate-limited bacteria with C surplus, C allocation to NLFA rather with reserve storage in C-limited higher microorganisms such as fungi. Potentially, similar dynamics drive the reported accumulation of TAG under N limitation in certain bacteria (Scott and Finnerty, 1976; Alvarez et al., 2000). In summary, the complex interplay between polar and non-polar lipids offers profound insights into the adaptive strategies and functional dynamics of microbial communities, particularly in response to nutrient limitations and environmental complexities (Bale et al., 2021; Couvillion et al., 2023; Zhang et al., 2023).

1.3. Hypothesis

In this study, we explored microbial community functioning in relation to nutrient and energy availability focusing on the N acquisition by free-living diazotrophs in relation to two distinct energy sources. We used $^{15}N_2$ labelling to incubate soils with natural gradients of degradation-requiring SOM in parallel with highly bioavailable artificial root exudates. We investigated microbial community functions using IPLs isolated from the soil. We hypothesise that (i) under low SOM availability in less fertile soils, artificial root exudates will provide an energy source for the soil microbial community, strongly stimulating N_2 fixation by diazotrophs. However, large parts of the microbial community require transformation processes to access the *de novo* fixed N. Therefore, (ii) we expect the bioavailable energy to cause microbial growth primarily through N-free energy-storage (e.g., TAG) and N-free membrane lipids (e.g., CL, PI, DGDG), indicating N limitation. In contrast, without bioavailable root exudates as a preferential energy source, free-living diazotrophs and the microbial community are dependent on SOM mineralisation. Thus, (iii) natural organic matter-rich soils support higher N-fixation and increased microbial biomass through N and P holding structural IPLs, such as phospholipids (e.g., PC, PE) and amino lipids (e.g., OL, betaine lipids).

2. Materials and methods

2.1. Study site and soil sampling

In our study, we used an Eutric Fluvisol from Jena, Germany (50°57′04.1″N 11°37′14.3″E, alt. 130 m NN), in the floodplain of the river Saale (FAO, 1997; Roscher et al., 2004), characterised by a strong texture gradient. To account for this texture gradient, the experimental site was arranged in four blocks of comparable soil texture (Table S1), with a total of 80 grassland plots, 6 × 6 m in size. These grassland plots provided a plant productivity gradient that was replicated in all blocks. Since site establishment, plant productivity slowly compensated for initial differences in SOM content due to the variations in soil texture and properties (block). Moreover, the productivity gradient resulted in a long-term gradient in SOM (Lange et al., 2015, 2023), ranging from 1.66 to 3.78% soil organic carbon (SOC) and from 0.12 to 0.33% total soil N. Soil sampling took place between the end of May and the beginning of June 2021. For each plot, we sampled soil from 0 to 5 cm of depths in triplicates. We mixed these triplicates to account for the spatial heterogeneity in soils. In addition, we sorted out all visible roots and sieved the soil to a grain size diameter of 2 mm. All samples were stored at -20 °C and allowed to acclimate to room temperature overnight prior to the processing in September 2021. Lipid-related analyses were completed in November 2021, bulk ^{15}N and total soil nitrogen analyses in June 2022. Besides our *de novo* analyses, our study utilised SOC and

the soil dry density at 5 cm of depth analysed at the experimental site in 2020, in addition to soil texture data analysed in 2002 (Lange et al., 2023).

2.2. $^{15}N_2$-soil incubation and calculation of the plant available water content

We incubated 0.9 g soil from each plot in 12 mL glass vacutainers. In addition, we established a highly bioavailable C input treatment to investigate the effect of an increased energy availability through root exudation in rhizospheric hotspots on FLNF and the microbial community. Therefore, we prepared an aqueous, pH-neutral solution that provided C in the form of sugars and organic acids, namely glucose, sucrose, citric acid, mannitol, malic acid and lactose-monohydrate (detailed information in Supp. 1). We added 268.75 μL of either the undiluted solution, a 50% dilution or ultra-pure water to the vacutainer. This corresponded to 8.6, 4.3 and 0.0 mg C, which upscaled equalled an average C input of 5.2 ± 0.4, 2.6 ± 0.2 and 0.0 kg C ha^{-1} respectively. These mimicked estimated C inputs to the rhizosphere (Angst et al., 2016) and partially saturated the soil with liquid, reaching approximately 80 ± 5% of the water holding capacity, which is in the range recommended by previous studies (Gupta et al., 2014; Smercina et al., 2019b). We used the control treatment (0.0 mg C input) to investigate the potential N uptake by FLNF based on the naturally available C sources in the soils, and thus we refer to it as the "soil potential for FLNF". The vacutainers were sealed airtight and we replaced 5.8 mL air with 6.0 mL $^{15}N_2$ (98 atom% ^{15}N, Sigma-Aldrich) or N_2 in natural abundance using air tight syringes. Using duplicates, we incubated a total of 960 samples in the dark at room temperature for 3 days. This experimental design, with dark incubation of soils and negligible residual plant biomass, ensured that changes in the soil lipidome were either of microbial origin or attributed to (physicochemical) transformation and degradation processes. After incubation, we dried the samples at 40 °C for ~3 days and milled them for 3 min at 25 Hz with two Ø5 mm steel beads in 2 mL Eppendorf vials using a TissueLyser Adapter (Qiagen) and a ball mill (MM 400, Retsch).

In our soil incubations, we kept the amount of soil and the volume of liquid added constant across the SOM gradient and the variable soil texture (blocks) of our experimental site. This introduced a soil property effect to our experiment, e.g., through a positive correlation between SOM and the soil water holding capacity (Libohova et al., 2018). To account for this effect, we calculated the soil water holding capacity as the plant available water content (AWC). Therefore, we first determined the water content of our soils at field capacity θ_{FC} (matrix potential = 6.8 (-kPa)) and at the permanent wilting point θ_{WP} (matrix potential = 1500 (-kPa)) with the pedotransfer function of Zacharias and Wessolek (2007) using dry density and soil texture data from our site (Lange et al., 2023). We used θ_{FC} and θ_{WP} in formula (1) to calculate the AWC.

$$AWC = \theta_{FC} - \theta_{WP} \quad (1)$$

2.3. Bulk ^{15}N and total soil nitrogen analyses

For ^{15}N and total soil N analyses, we weighted 25–35 mg of bulk soil into tin capsules and analysed them with an elemental analyser (NA1100, CE Instruments) coupled to an isotope ratio mass spectrometer (Delta + XL, Thermo Finnigan) via an interface (ConFlowIII, Thermo Finnigan). We obtained a single estimate per experimental unit by averaging the duplicates. We calculated $\delta^{15}N$ values (for ‰ *1000) according to formula (2) with the isotope ratios ($^{15}N/^{14}N$) of the samples and internal standards (Supp. 2).

$$\delta^{15}N = \left(\frac{\left(\frac{^{15}N}{^{14}N}\right)_{sample}}{\left(\frac{^{15}N}{^{14}N}\right)_{standard}} \right) - 1 \quad (2)$$

Natural abundance samples were treated as controls. Thus, we corrected the labelled samples against the natural abundance background and calculated $\Delta\delta^{15}N$ values according to formula (3).

$$\Delta\delta^{15}N = \delta^{15}N_{Labelled\ sample} - \delta^{15}N_{Natural\ abundance\ background} \quad (3)$$

We used the $\Delta\delta^{15}N$ values to calculate the potential annual N uptake by FLNF into the soils in three steps. Firstly, we calculate the corresponding atom% (AP) ^{15}N values with formula (4), where ^{15}N or ^{14}N represents moles of the N isotope, and secondly, the atom%excess (APE) ^{15}N, with formula (5), where $AP^{15}N_{control}$ represents the AP of the control plots that were incubated with natural abundance air (AP = 0.36782) (IAEA, 2009; Brand and Coplen, 2012; Meija et al., 2016).

$$AP\ ^{15}N = \left(\frac{^{15}N}{^{15}N + ^{14}N} \right) * 100 \quad (4)$$

$$APE\ ^{15}N = AP^{15}N_{Sample} - AP^{15}N_{Reference} \quad (5)$$

Thirdly, we used the APE ^{15}N values with the analysed total soil N to calculate the ^{15}N concentration in our soil samples, followed by the potential ^{15}N uptake by FLNF with formula (6) (adapted, Schrumpf et al., 2011). Here BD is the soil density, analysed in 2020 as dry density of each plot (Lange et al., 2023), and LT the layer thickness, in our case the top 5 cm of soil equal to our sampling depths. As FLNF is primarily driven by root exudation (Smercina et al., 2019a), which peaks during the main vegetation period (Gao et al., 2023), we present the potential annual ^{15}N uptake by FLNF (in kg N ha^{-1}) in the topsoil (5 cm) with formula (7) on the basis of the main exudation period of 60 days (Strobel, 2001).

$$^{15}N\ uptake_{FLNF}\left[\frac{g}{m^2}\right] = {}^{15}N\ concentration\left[\frac{g}{kg}\right] * BD\left[\frac{g}{cm^3}\right] * LT\ [cm] * 10 \quad (6)$$

$$Pot.\ ann.\ ^{15}N\ uptake_{FLNF}\left[\frac{kg}{ha}\right] = \frac{^{15}N\ uptake_{FLNF}\left[\frac{g}{m^2}\right] * 10 * 60\ [d]_{exudation\ period}}{3\ [d]_{incubation\ period}} \quad (7)$$

We identified and removed two outliers in the total soil N measurements using a Rosner's test (Rosner, 1983), which did not affect our results. To match the scale of the potential annual ^{15}N uptake, we calculated the average C input per hectare (kg C ha^{-1}) using formula 5, replacing the term ^{15}N concentration with our C input (in g C kg_{soil}^{-1}).

2.4. Lipid extraction

For lipid extractions and analyses we subsampled incubated soils from 11 plots. These subsamples were representative of the plant productivity gradient and therefore for all plots in our study. All subsamples were gained from one block, which ensured consistent soil texture and microbial community composition (Dassen et al., 2017). Our subsampling maintained the SOM gradient and the C input treatment for both the $^{15}N_2$ and natural abundance N_2 aliquots, resulting in a total of 66 extracted samples for the lipidome analysis. We included one extraction blank in each lipid extraction run, approximately one in every 8 samples extracted. Lipid extraction was based on a modified Bligh-Dyer protocol including two buffer solutions (Sturt et al., 2004; Wörmer et al., 2015; Bale et al., 2021). In short, buffer 1 was created with methanol (MeOH, HiPerSolv Chromanorm for HPLC LC-MS, VWR), dichloromethane (DCM, SupraSolv for GC-MS, Supleco) and aqueous di-potassium hydrogen phosphate (K_2HPO_4, for HPLC, Supleco; approximately 8.7 g per L water) solution (2:1:0.8, V:V:V, pH 7.4). Buffer 2 consisted of MeOH, DCM and aqueous trichloroacetic acid (TCA, AnalaR Normapur, VWR; approximately 50 g per L water) in the ratio 2:1:0.8 (V:V:V, pH 2.5). We extracted 0.7 g of the incubated soil, including 50 ng 1,2-dinonadecanoyl-sn-glycero-3-phosphocholine (PC-DAG (19:0_19:0), Avanti) as an internal standard. For each buffer,

starting with buffer 1, we sequentially extracted the samples twice with 3 mL buffer solution in a sonicator for 10 min. We collected the supernatants, mixed and centrifuged (30 s at 2000 rpm) them twice with additional dichloromethane (DCM) and aqueous K_2HPO_4 or aqueous TCA, respectively (final solvent ratio 1:1:0.9, V:V:V), collecting the organic phase sequentially. For each sample, we combined all organic phases into a total lipid extract, which we evaporated under a gentle stream of N_2. We took 2 mg (dry weight) aliquots for analysis and stored all samples at −20 °C until analysis.

2.5. LC-MS/MS analysis and feature based molecular network

Prior to analysis, we spiked all total lipid extracts with 1,2-dipalmitoyl-sn-glycero-3-O-4'-[N,N,N-trimethyl(d9)]-homoserine (DGTS-d9, Avanti) as internal standard and filtered them to 0.45 μm. We used ultra-high-performance liquid chromatography-high-resolution mass spectrometry (UHPLC-HRMS, 1290 Infinity II, Agilent & Q Exactive Orbitrap MS, Thermo Fischer Scientific) with the reverse phase method of Wörmer et al. (2013). The settings used for the UHPLC-HRMS analysis and the subsequent data conversions are described in detail in Bale et al. (2021) and Ding et al. (2021). In short, for the UHPLC we used a C18 column (Acquity BEH C18, Waters, 2.1 × 150 mm, 1.7 μm) at 30 °C with 3 min 95% eluent A: methanol/water/formic acid/14.8 M NH_3aq (85:15:0.12:0.04, V:V), linearly decreasing to 40% A at 12 min and 100% eluent B: propan-2-ol/methanol/formic acid/14.8 M NH_3aq (50:50:0.12:0.04, V:V), maintained from min 50 till the end at min 80. We used the HRMS in positive mode with a mass range of 350–2000 *m/z*, with subsequent tandem MS/MS and a dynamic exclusion of repeating masses. We converted the output data into mzXML-files with MSconvert (Chambers et al., 2012). Following Ding et al. (2021) we extracted MS^1 and MS^2 spectra with MZmine 2.53 (Pluskal et al., 2010) and performed the subsequent processing including mass peak detection, chromatogram building and deconvolution, isotope grouping, feature alignment, row and isotope filtering and gap filling (Wang et al., 2016). Peak threshold was set to $5e^5$, the peak duration to 0.05–5.00 min during deconvolution and the baseline level to $8e^4$. We used the Global Natural Product Social Molecular Network (GNPS) (Wang et al., 2016) and the tool for Feature Based Molecular Networking (FBMN) (Nothias et al., 2020) to process the dataset as described earlier (Ding et al., 2021). To minimise dilution effects and exclude potential contaminants, we subtracted solvent and extraction blanks, and normalised sample intensities with the internal standard. FBMN greatly facilitated lipid identification, as molecules were clustered by their structural similarities based on their fragmentation patterns. The network consisted of 16766 features in 1507 clusters and was visualised with Cytoscape 3.9.0 (Shannon et al., 2003).

2.6. Lipid identification, data selection and analysis

Besides some lipid hits with the GNPS library, we tentatively identified lipids in the clusters of the molecular network by manual inspection of the MS^2 spectra, accepting a mass deviation threshold of 3 ppm from the expected mass of a compound. We re-evaluated the manual lipid identification with SIRIUS (Dührkop et al., 2019), the inbuilt CSI: FingerID (Hoffmann et al., 2021) and CANOPUS (Dührkop et al., 2021). During data processing, we sorted the identified lipids by intensity and filtered the 20 most abundant lipids from each identified lipid class for statistical analysis. For classes with fewer than 20 species, all lipids were included, resulting in a total of 222 lipid species from 22 lipid classes for further analysis (Table S3: # of lipids). We ensured semi-quantitative comparability between the lipid classes by using external standards to normalise for their different ionisation response in our mass spectrometer (Ding et al., 2024, and their Supplementary Tables 1 and 2). In short, for each lipid class, a single representative lipid was analysed to calculate a response factor in comparison to our internal standard DGTS-d9, which had the highest response with $1.58e^9$ [Peak area/ng organic C] (Table S5). We used the resulting response factors of each lipid class to calibrate our lipid peak intensities in a one-point calibration with formula (8). Lipid classes without equivalent or structurally comparable external standard (e.g., cardiolipins (CL), chlorophylls and quinones) were calibrated with an average response factor for all lipid classes. All lipid related data and figures presented in this manuscript are based on calibrated lipid intensities.

$$Lipid\,intensity_{Cal}\left[\frac{Peak\,area}{g\,soil}\right]=\frac{Analysed\,lipid\,intensity\left[\frac{Peak\,area}{g\,soil}\right]}{Response\,factor\,of\,the\,representative\,standard} \quad (8)$$

We investigated general changes in the microbial biomass with C source bioavailability and degradability using the summed abundance of all structural membrane lipids (betaine lipids, ceramides, CL, DGDG, hopanoids, lyso-PC, MMPE (monomethyl-phosphatidylethanolamine), OL, PC, PE, PG (phosphatidylglycerol), PI (phosphatidylinositol)) and non-structural lipids in our data set (acyletherglycerol (AEG), chlorophyll, diacylglycerols (DAG), dietherglycerols (DEG), Quinone, Wax and fatty acid ester). Further, we used TAG, a typical microbial storage compound, and the response of individual cell membrane building IPL (e.g, PE, PC, hopanoids, OL and betaine lipids) to distinguish between biomass growth with low and high replication. For insights into the microbial community's nutritional status reflected by e.g., membrane adjustments, we analysed changes in the proportion of P- and N-free glycero- (AEG, DAG, DEG, DGDG, TAG), P-free amino- (betaine lipids, ceramides, OL), N-free (CL, PG, PI) and N-containing phospholipids (MMPE, PE, PC).

In our study, we did not correlate the lipid data with the investigated ^{15}N uptake, to avoid false correlations by chance. This is because lipids were derived from the entire soil microbial community, whereas ^{15}N uptake was limited to FLNF by a specific, minor subset of this community. In addition, the applied method was designed for an untargeted screening of various lipid classes. It is limited in the detection of component-specific ^{15}N enrichment to exclusively highly labelled and concentrated N containing lipid species. In our study, however, a potential ^{15}N enrichment of *de novo* synthesised N containing lipids by free-living diazotrophs is masked by the total soil microbial community yielding unlabelled equivalents.

2.7. Statistics

To investigate the effect of the C input and the natural SOM gradient on the ^{15}N uptake through free-living diazotrophs, we performed Linear Mixed-Effects Models (LMM) using the "lmer" function of the R package "lme4" (Bates et al., 2015). The ^{15}N uptake values were log-transformed. We started from a constant null model (M0) with plot as random intercept, which accounted for the repeated measurements of each plot due to the 3 levels of our C input treatment. This null model was stepwise extended (Supp. 3). Following Lange et al. (2021), we fitted block (M01) as fixed effect, since the blocks are arranged in a linear sequence from the river, and thus do not meet the normal distribution assumption of a random effect (Schmid et al., 2017). We found that block accounted for >50% of the AWC effect on the ^{15}N uptake (Table S2). To consider the full effect, we fitted the next fixed terms in the following sequence: AWC, C input, SOC gradient. We fitted SOC last, as it was the weakest effect in our tests (Table S2). For model comparison and to test for significant model enhancement with each fixed effect, we used likelihood ratio tests (reported Chi^2) (Zuur et al., 2009). SOC and the total soil N were highly correlated in our experimental site (Fig. S1). Thus, we tested for the total soil N and the CN ratio in separate models, replacing SOC in the fitting sequence.

To investigate the effect of the C input and the natural SOM gradient on the microbial lipid abundances in the soils, we log transformed the lipid intensities. All extracted lipid samples originated from the same

block of the experimental site, which renders the first fixed effect block in our LMM, obsolete. During sample processing, $^{15}N_2$ labelled and the natural abundance samples were processed in spatially separated laboratories to avoid cross-contamination. This laboratory separation caused small changes in lipid abundances, which were unrelated to a potential ^{15}N enrichment in specific N containing lipids of free-living diazotrophs. We accounted for this laboratory related variability by fitting "batch" as the first fixed effect. The sequential fitting order of the fixed terms remained as described before (AWC, C input and then SOC gradient). To investigate the relation between microbial energy storage, structural and non-structural biomass we selectively expanded the model by e.g., "structural membrane lipids" as covariate. Besides the LMM, we performed t-tests to test for significant changes between the potential annual ^{15}N uptake with the intermediate and high C input treatment. We performed similar tests further investigating the effect of the SOM gradient and AWC on the ^{15}N uptake by establishing 3 equally sized discrete groups (SOC: low $\leq$ 2.31%, intermediate $\leq$ 2.77%, high >2.77%, total soil N: low $\leq$ 0.22%, intermediate $\leq$ 0.25%, high >0.25%, AWC: low $\leq$ 0.260, intermediate $\leq$ 0.281, high >0.281 cm^3cm^{-3}). We used Principal Coordinates Analysis (PCoA) with Bray-Curtis dissimilarity of the R package "vegan" (Oksanen et al., 2022) to explore the compositional lipid data. We chose PCoA over Principal Component Analysis (PCA) due to PCoA's advantageous performance with double zeros (Ramette, 2007), common in HPLC-MS/MS data.

3. Results

3.1. Free-living nitrogen fixation

A high soil potential for FLNF (control) was observed that increased the soils $\Delta\delta^{15}N$ values on average by 1226.4 ± 360.2‰, corresponding to a potential annual ^{15}N uptake of 111.4 ± 35.5 kg N ha^{-1} (Fig. 1). The FLNF potential was further increased by 555.1‰ following the input of bioavailable C in the form of sugars and organic acids, corresponding to an additional potential annual ^{15}N uptake of 51.3 kg N ha^{-1} on average ($Chi^2 = 92.3$, $P < 0.001$, Fig. 1). We observed no significant difference in the ^{15}N uptake between the intermediate and high C input, even if it was slightly higher in the latter (+8.5 kg N ha^{-1}). The soil potential for FLNF (control) was higher in SOM rich soils. However, the effect of C input on the additional ^{15}N uptake in SOM poor soils exceeded the additional ^{15}N uptake in SOM rich soils by 20.2 kg N ha^{-1} ($P < 0.05$), thus equalising the SOM effect observed in the control. SOM and the total soil N were highly correlated at our experimental site (Pearson $R = 0.78$, $P < 0.001$, Fig. S1). In addition, we found a significant negative effect of the CN ratio on the ^{15}N uptake in the control (Fig. S2). Note that the plant available water content (AWC) was significantly higher in soils with coarser texture and positively correlated to SOM in most blocks of our experimental site (Fig. S3). We found a significant negative effect of AWC on the ^{15}N uptake ($Chi^2 = 10.2$, $P < 0.01$) in the control samples, which was negated by C input, similar to the effect of SOC, TN and CN. We accounted for this effect in our LMM.

3.2. Soil lipid composition

The variability of the lipid composition in our samples was predominantly driven by the input of highly bioavailable C (primarily on the PC 1 axis with 65.1% of the total variability) and to a lesser extent by SOM (PC 2 axis with 9.6% of the total variability), here further investigated as SOC (Fig. 2). Highly bioavailable C stimulated lipid synthesis and thus the microbial biomass in general. This was reflected in the absolute intensity of structural membrane lipids increasing 2.2-fold ($Chi^2 = 125.5$, $P < 0.001$), non-structural lipids increasing 2.5-fold ($Chi^2 = 111.0$, $P < 0.001$) and energy-storage related TAG increasing 2.3-fold ($Chi^2 = 88.8$, $P < 0.001$) on average with the highest C input (Fig. 3, Table S3). TAG and structural membrane lipids were positively correlated ($Chi^2 = 24.2$, $P < 0.001$), their ratio remained unchanged by C input (Fig. 4A). However, the response of the microbial lipid synthesis to highly bioavailable C varied between the investigated major lipid classes. From a macronutrient perspective, C input caused a shift towards a N- and, to a lesser extent, P-free microbial biomass (Fig. 4B). We observed a preference for P- and N-free glycerolipids ($Chi^2 = 133.9$, $P < 0.001$) and N-free phospholipids ($Chi^2 = 106.8$, $P < 0.001$) over N-containing phospholipids ($Chi^2 = 29.2$, $P < 0.001$) and aminolipids ($Chi^2 = 13.4$, $P < 0.01$).

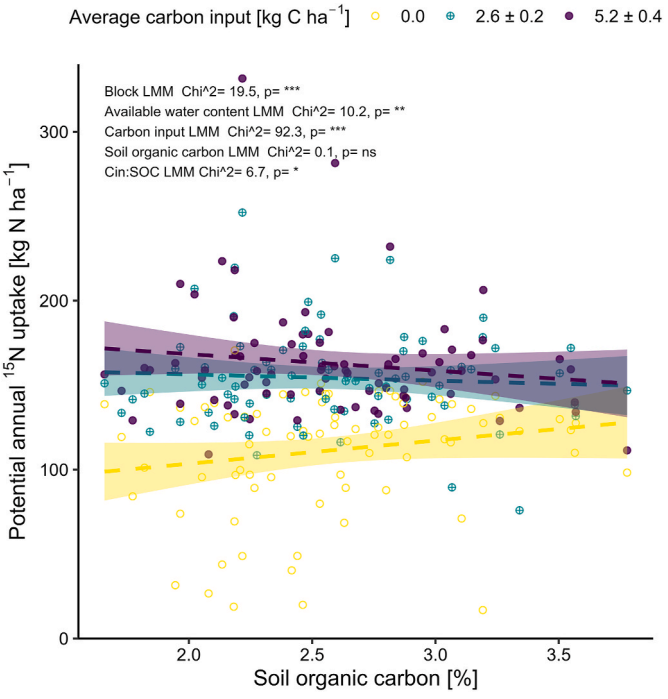

Fig. 1. The effect of soil organic carbon (SOC) coloured according to the carbon (C) input (upscaled) on the potential annual ^{15}N uptake during the soil incubations with the ANOVA results of the Linear Mixed-Effects Models.

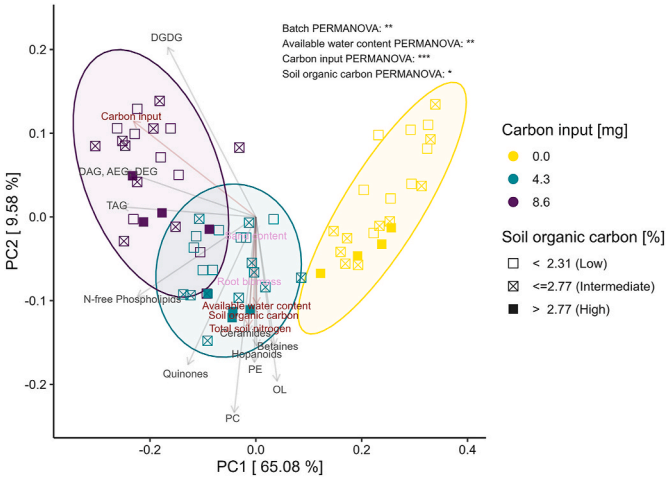

Fig. 2. Principal Coordinates Analysis (PCoA, using Bray-Curtis dissimilarity), based on the calibrated intensities of the individual lipids filtered from the soil lipidome with PERMANOVA results. Squares represent individual samples, coloured according to the carbon input treatment with shapes representing the soil organic carbon gradient. Ellipses coloured according to the carbon input assume a multivariate t-distribution. The vectors indicate the effect of the environmental factors inherent to the experimental site and the carbon input treatment (red, not significant: pink) and the behaviour of the summed intensity of selected lipid groups (dark grey).

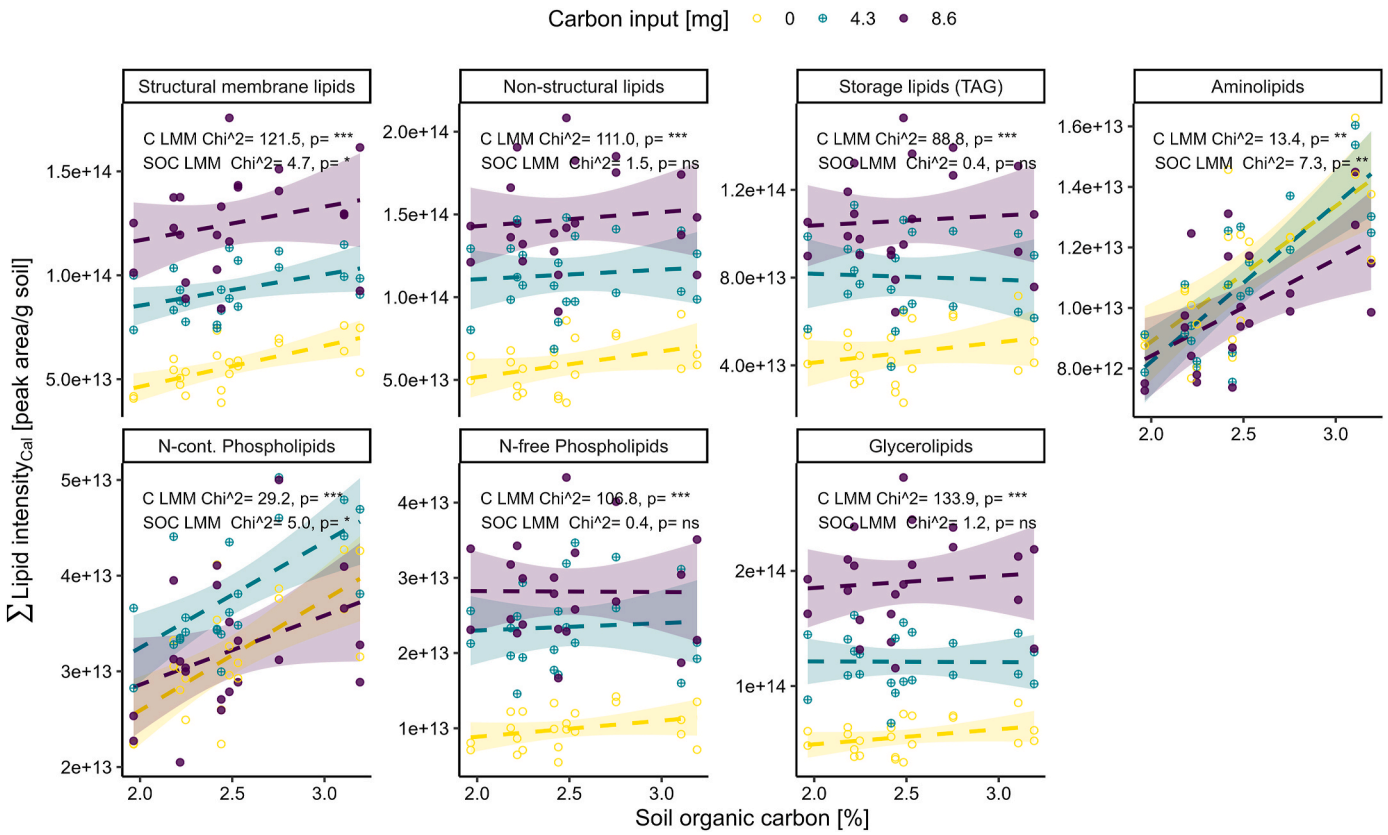

Fig. 3. The effect of soil organic carbon (SOC) on major lipid class composition, coloured according to the carbon (C) input on the summed (Σ) calibrated intensity of A) structural membrane lipids; B) non-structural lipids; C) storage lipids; D) aminolipids; E) N-containing phospholipids; F) N-free phospholipids and G) N & P-free glycerolipids including the ANOVA results of the Linear Mixed-Effects Models. Lipids included are A) betaine lipids, ceramides, CL, DGDG, hopanoids, lyso-PC, MMPE, OL, PC, PE, PG, PI; B) AEG, chlorophyll, DAG, DEG, Quinone, Wax and fatty acid ester; C) TAG; D) Betaine lipids, Ceramides, OL; E) PC, Lyso-PC, PE, MMPE; F) PG, CL, PI and G) AEG, DAG, DEG, DGDG, TAG.

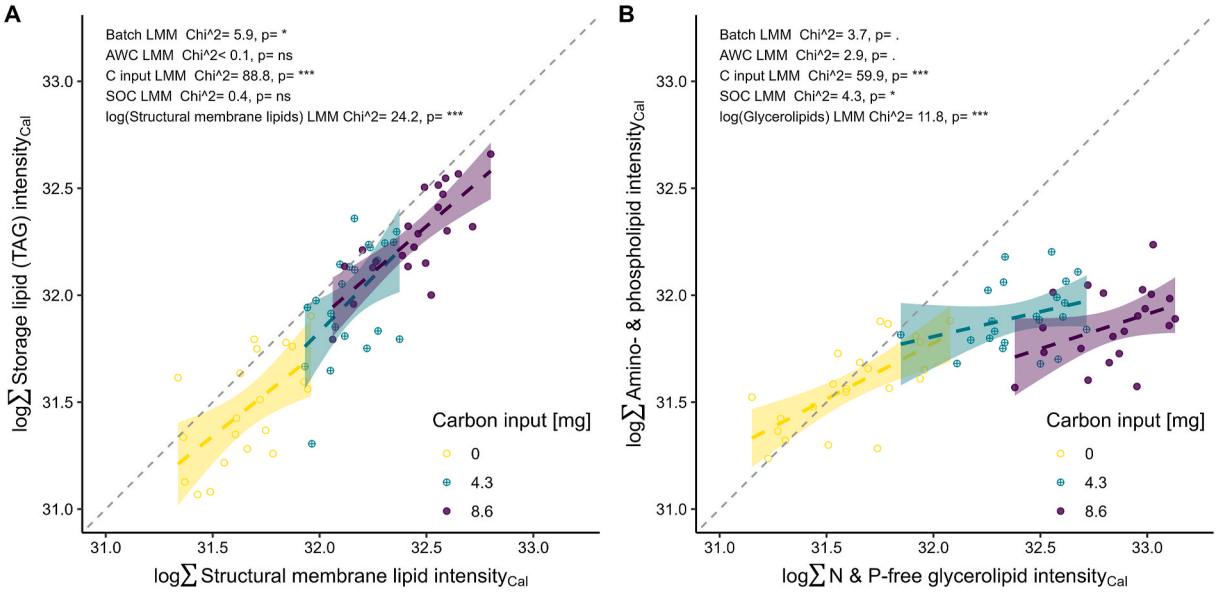

Fig. 4. The relation between the log transformed summed calibrated intensity of A) storage lipids and structural membrane lipids B) amino and phospholipids versus N and P-free glycerolipids, coloured according to the carbon (C) input, also showing the ANOVA results of the Linear Mixed-Effects Models (LMM).

Besides the synthesis of energy-storage related TAG, DGDG –also a P-free and N-free glycerolipid class– increased 27-fold with the high C input (Chi^2 = 188.8, P < 0.001, Fig. 5, Table S3). This represented a substantial increase in the relative contribution of DGDG to the total pool of the investigated lipid classes, rising from 1.7 ± 0.5% under control conditions to 19.3 ± 5.2% with high C input (Table S4). Less abundant N-free phospholipids such as CL (Chi^2 = 136.1, P < 0.001), PG-DAG (Chi^2 = 112.1, P < 0.001), and PI-DAG (Chi^2 = 76.1, P < 0.001)

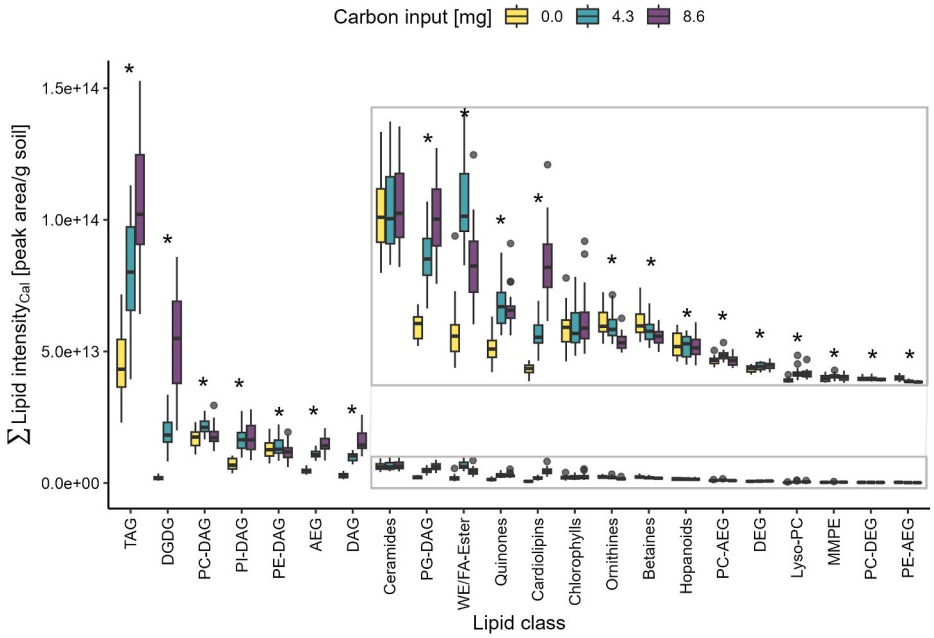

Fig. 5. The effect of highly bioavailable carbon input on the summed calibrated intensity of the investigated lipid classes with stars representing significance from the ANOVA results of the Linear Mixed-Effects Models. The grey rectangle marks the enlarged section with intensities (y-axis) between 0 and 1.0e^{+13}.

were increased as well. Major N-containing phospholipids e.g., PC-DAG ($Chi^2 = 38.7$, $P < 0.001$) and PE-DAG ($Chi^2 = 8.5$, $P < 0.05$) showed a maximal increase with the intermediate C input (Fig. S4). Whereas aminolipids, such as OL ($Chi^2 = 81.5$, $P < 0.001$) and betaine lipids ($Chi^2 = 35.5$, $P < 0.01$), but also hopanoids ($Chi^2 = 8.0$, $P < 0.05$), which were mostly N containing (adenosyl-)hopanoids, were negatively affected.

Comparing low (<2.31%) and high (>2.77%) SOC soils, higher SOC content was accompanied by a minor increase in structural membrane lipids by ($Chi^2 = 4.7$, $P < 0.05$) (Fig. 3, Table S3, Fig. S5A). Contrary to C input, higher SOC affected the lipid abundance by primarily increasing N-containing lipids like aminolipids ($Chi^2 = 7.3$, $P < 0.01$) and N-containing phospholipids ($Chi^2 = 5.0$, $P < 0.05$) (Fig. 3, Fig. S5B). Thus, major N containing membrane lipids, e.g., PE-DAG, PC-DAG, OL, Betaine lipids and (adenosyl-)hopanoids were generally positively affected by SOC (Table S3, Fig. S4). However, energy-storage related TAG, but also DGDG, were not positively affected by the SOC gradient, a contrast to the strong increase observed with the highly bioavailable C input. Although we fitted AWC before C input and SOC in our LMM, AWC had only a marginal effect on lipid abundances (Table S3). Any effect, such as a positive correlation with N-containing phospholipids ($Chi^2 = 4.7$, $P < 0.05$), was accounted for in our models.

4. Discussion

4.1. N_2 fixation

4.1.1. High natural potential for FLNF in our experimental site

We identified a high soil potential for FLNF (no addition of artificial exudates) in the topsoil of our experimental site corresponding to an estimated N uptake of 111.4 kg N ha^{-1}y^{-1} (Fig. 1). The high N uptake we observed is comparable to the levels of N fertiliser used in managed grasslands (Weigelt et al., 2009). This underscores the significance of free-living nitrogen fixation (FLNF) as a potentially important source of N in terrestrial environments (Smercina et al., 2019a). However, the high soil potential for FLNF in our experimental site was also surprising, as the realised N storage in our soils was reported to be in the range of 30–35 kg N ha^{-1}y^{-1} (Weisser et al., 2017) and FLNF in temperate grasslands was generally expected to contribute N in the range of 0.1–21 kg N ha^{-1}y^{-1} (Reed et al., 2011). Note that the realised N storage reported in Weisser et al. (2017) refers to the first years after the experiment was established on a former arable field with high fertiliser inputs and that during this time changes in the N cycle were observed (Oelmann et al., 2011). Almost 20 years after the establishment of the experiment, without fertiliser addition and removal of harvested plant biomass a changed plant-microbial interaction is assumed to maintain soil functioning and plant productivity (Lange et al., 2019). Furthermore, we only assumed a main root exudation period of 60 days (Strobel, 2001) as the period of the main FLNF activity, for our calculation of the annual potential ^{15}N uptake, although it can be assumed that FLNF is performed beyond this time. In addition to the gaseous losses and N leaching not considered here, the management of the unfertilised experimental site as a meadow with N removal by annual plant harvesting likely created periodic conditions of N demand in our soils, generally assumed to increase the potential for FLNF (Reed et al., 2011). Further, the potential N uptake in our *in vitro* soil incubations expectedly exceeded the realised N uptake under *in situ* conditions, as our experimental design ensured favourable conditions for FLNF. This included energy supply, temperature, oxygen limitation, and water saturation, creating both aerobic and anaerobic microsites in the soils (Smercina et al., 2019a).

4.1.2. Greater N_2 fixation increases in SOM poor soils

In line with our hypothesis (i), the microbial community used highly bioavailable energy, like the provided artificial root exudates, to increase FLNF, equalling an additional N uptake of 51.3 kg N ha^{-1}y^{-1} in the topsoil (Fig. 1). The promoting effect was quantitatively higher in SOM poor soils, suggesting both a stronger energy limitation of FLNF in SOM poor soils, confirming C availability as an important driver (Gupta et al., 2014), and an initially better performing free-living diazotrophic community on the existing more complex energy sources with less additional fixation from highly bioavailable energy. Our findings indicate that an increase in root exudation, putatively caused by more diverse plant communities (Eisenhauer et al., 2017) will reduce the energy limitation for FLNF in the rhizosphere, likely increasing its potential, especially in SOM poor ecosystems. In addition, we can expect a high potential for FLNF in certain ecosystems already today, as the input of root exudates e.g., in the grasslands of the Inner Mongolia during the

growing season with 4–19 g C m^{2-1} per month (Shen et al., 2020) resembles the quantities of the inputs in our study when calculated per month with approximately 7.8 ± 0.6 g C m^{2-1} and 15.6 ± 1.3 g C m^{2-1}.

4.1.3. Saturation of the additional N_2 fixation

However, our data indicated a saturation of the additional N uptake by FLNF by highly bioavailable energy input (Fig. 1), suggesting a saturation of FLNF energy requirements within the three days of our study. Besides a saturation in energy, the potential of FLNF could have been limited by another driver not further investigated here. For example, Zheng et al. (2023) showed that the energy-intensive FLNF (de Bruijn, 2015) is reduced in the presence of existing N stocks on a global scale, with reasons discussed including a reduction in facultative N_2 fixation (Gutschick, 1981) or a reduction in the biosynthesis of the enzyme nitrogenase, required for N_2 fixation (Bentley, 1987).

4.1.4. Microorganisms prefer bioavailable C over SOM

In line with hypotheses (iii), SOC and thus SOM rich soils had on average a 20.2 kg N ha^{-1} ($P < 0.05$) increased soil potential for FLNF (control) (Fig. 1), suggesting that heterotrophic N-fixers (and the microbial community) in SOM rich soils used the higher energy availability from the degradation of SOM to gain additional N through FLNF. This finding highlights SOM degradation as an energy source for heterotrophic FLNF (Reed et al., 2011; Zheng et al., 2020). However, we did not observe an additional increase in the N uptake by FLNF in SOM rich soils with simultaneous input of C (Fig. 1). Thus, in the interplay of both energy sources, free-living diazotrophs preferred the highly bioavailable artificial root exudates, over the degradation requiring SOM as energy source.

4.2. Lipids derived from the soil microbial community

4.2.1. Accumulation of N-free lipids with bioavailable energy indicates nutrient limitation

Highly bioavailable energy from the input of artificial root exudates was used by the soil microbial community for biomass growth, indicated by a more than twofold increase in structural membrane lipid abundance (Fig. 3), which was furthermore accompanied by a strong shift in the lipid composition (Fig. 2). In line with hypothesis (ii), biomass growth was primarily achieved through the synthesis of N-free phospholipids (e.g., PI, PG, CL) and glycerolipids (e.g., DGDG), including storage-related TAG, which serve as markers of non-stoichiometric biomass growth, rather than through N-containing lipids (e.g., PE, PC, OL, betaine lipids, adenosylhopanoids) (Fig. 4, Table S3, Table S4, Fig. S4). Adaptation of the lipidome with a dominant synthesis of N-free lipids likely indicated a microbial response to N limitation. Microbial N limitation would be in line with previous results from our experimental site, where the site was found to be limiting by N rather than by P in general (Weisser et al., 2017). However, our results also showed that the supplied highly bioavailable energy was used by the free-living diazotrophs in the soil for an increased N uptake (Fig. 1). Hence, we observed the highest N_2 fixation in a presumably more nutrient limiting system, as the lipids derived from the microbial community were C-rich, but low in N (and to a lesser extent in P). In addition, the preferential synthesis of N-free lipids suggests, that large parts of the microbial community were unable to access the *de novo* fixed N without further transformation processes of the necromass from the diazotrophs on a short time scale, or that the quantities of fixed N were insufficient to balance the available C for substantial cellular growth based on N containing membrane lipids (microbial stoichiometry: Zechmeister-Boltenstern et al., 2015).

4.2.2. Bioavailable energy causes microbial biomass growth without additional storage

Although considerable quantities of the microbial biomass growth in our soils were caused by the synthesis of storage compounds in response to C input (Mason-Jones et al., 2023), the parallel synthesis of N-free membrane lipids kept the ratio of storage to structural biomass stable throughout the C treatment (Figs. 3 and 5). This equal increase in storage and cellular growth suggests that the microbial community in our soils used TAG primarily for reserve rather than surplus storage, which is consistent with recent studies (Butler et al., 2023; Mason-Jones et al., 2023). TAG synthesis continued to increase between the intermediate and the high energy inputs (Figs. 3 and 5), which contrasts the observed N uptake (Fig. 1). This finding may indicate that FLNF experiences energy saturation prior to energy storage.

Energy storage with TAG is mainly known for eukaryotes such as fungi and some bacteria like *Actinobacteria*. Other bacterial taxa, such as *Proteo-*, *Cyano-* and *Actinobacteria* use PHB (Mason-Jones et al., 2022; Butler et al., 2023), which can make up a considerable proportion of storage compounds. In our study, however, the untargeted lipid screening method used was not optimised to analysing large oligomers such as PHB. Future studies should consider the whole set of energy storage compounds including TAG, PHB, glycogen and cyanophycin.

The stable ratio between storage and structural membrane lipids was primarily caused by the strong increase in membrane-related DGDG, with bioavailable energy in our soils (Fig. 5). As a result, DGDG became a major lipid class (Table S4). Since our experiment used plant-free soil and dark incubation, it excluded common sources of DGDG such as plants and other obligate phototrophs (Schubotz, 2019), hence making the increase in DGDG rather atypical for microbial cellular growth. We assume that the unexpected, but substantial increase in DGDG, and therefore the observed shift in membrane lipid composition, was provoked by the changing carbon/nutrient ratio with our carbon treatment. In this regard, DGDG could be attributed to certain bacteria (Brundish et al., 1966; Tatituri et al., 2012; Hines et al., 2017) that stabilise their membranes against N loss due to the recycling of N containing compounds. However, the observed increase in DGDG needs further investigation.

4.2.3. SOM increases cellular growth through N containing membrane lipids

In contrast to the strong increase in microbial biomass with highly bioavailable energy, we observed an expected (hypothesis iii) slight increase in IPL abundance and thus microbial biomass in SOC- and hence SOM rich soils (Fig. 3, Table S3). This positive effect of SOM on microbial biomass was consistent with previous findings on the experimental site (Prommer et al., 2020). SOM driven biomass growth was distinct from the growth with N-free structural membrane- and storage lipids due to highly bioavailable C, as SOM availability promoted cellular growth with major N-containing membrane lipids over storage (Fig. S4, Fig. S5, Table S3, Table S4). First, a preference for storage in low SOM, and thus less fertile soils is in line with the recent literature (Butler et al., 2023). Second, considering the positive effect of SOM on the potential N uptake by FLNF without C input (Fig. 1), our lipid data suggested that SOM rich soils harboured an abundant microbial community, which neglected storage and used available C to gain N from FLNF and existing SOM stocks in order to meet the microbial demand for growth (Zechmeister-Boltenstern et al., 2015).

5. Conclusion

Besides SOM decomposition, plant root exudates provide a major carbon and energy source for various soil microbial functions such as free-living N_2 fixation, cellular growth and storage. Our study identified root exudates as the primary energy source for an unexpected high potential free-living N_2 fixation in the soils of a long-term unfertilised temperate grassland. Simultaneously, large parts of the microbial community utilised root exudates to mineralise soil organic matter for cellular growth and storage rather than N_2 fixation. This underscores the critical role of organic matter decomposition for plant nutrition.

Our findings highlight the importance of non-symbiotic plant-microbial interactions in plant nutrition and nitrogen cycling. They

emphasise that plant-derived carbon and energy inputs into the soil are key factors in shaping soil microbial functions that are beneficial to plant growth. Our results have potential implications for the transition from nitrogen fertiliser-dependent agriculture to more sustainable nitrogen management in agriculture.

CRediT authorship contribution statement

Georg Dittmann: Writing – original draft, Visualization, Investigation, Formal analysis. **Su Ding:** Writing – review & editing, Methodology. **Ellen C. Hopmans:** Writing – review & editing, Methodology. **Simon A. Schröter:** Writing – review & editing. **Alice M. Orme:** Writing – review & editing. **Erika Kothe:** Writing – review & editing. **Markus Lange:** Writing – review & editing, Supervision, Conceptualization. **Gerd Gleixner:** Writing – review & editing, Supervision, Conceptualization.

Data availability

We will make data available as soon as the manuscript is accepted.

Declaration of competing interest

The authors declare that they have no known competing financial interests or personal relationships that could have appeared to influence the work reported in this paper.

Acknowledgment and funding

We like to thank Iris Kuhlmann, Heike Geilmann, Dr. Heiko M. Moossen, Akanksha Rai and Frederic D. Lange from the MPI-BGC in Jena for their help during soil sample preparation and ^{15}N analysis. Furthermore, we thank Nicole Bale, Anchelique Mets, Denise Dorhout and Monique Verweij from the NIOZ in Texel for support and training during the LC-MS/MS analysis. G. Dittmann thanks the International Max Planck Research School for Global Biogeochemical Cycles (IMPRS-gBGC) for funding his PhD studies. S.D. and E.C.H. were supported by the funding from the European Research Council (ERC) under the European Union's Horizon 2020 research and innovation program (grant agreement no.694569-MICROLIPIDS) awarded to Jaap S. Sinninghe Damsté. M. Lange gratefully acknowledges the support of the Zwillenberg-Tietz Foundation.

Appendix A. Supplementary data

Supplementary data to this article can be found online at https://doi.org/10.1016/j.soilbio.2025.109748.

References

Abida, H., Dolch, L.J., Mei, C., Villanova, V., Conte, M., Block, M.A., Finazzi, G., Bastien, O., Tirichine, L., Bowler, C., Rebeille, F., Petroutsos, D., Jouhet, J., Marechal, E., 2015. Membrane glycerolipid remodeling triggered by nitrogen and phosphorus starvation in Phaeodactylum tricornutum. Plant physiology 167, 118–136. https://doi.org/10.1104/pp.114.252395.

Alvarez, H.M., Kalscheuer, R., Steinbuchel, A., 2000. Accumulation and mobilization of storage lipids by Rhodococcus opacus PD630 and Rhodococcus ruber NCIMB 40126. Applied Microbiology and Biotechnology 54, 218–223. https://doi.org/10.1007/s002530000395.

Angst, G., Kögel-Knabner, I., Kirfel, K., Hertel, D., Mueller, C.W., 2016. Spatial distribution and chemical composition of soil organic matter fractions in rhizosphere and non-rhizosphere soil under European beech (Fagus sylvatica L.). Geoderma 264, 179–187. https://doi.org/10.1016/j.geoderma.2015.10.016.

Ashton, I.W., Miller, A.E., Bowman, W.D., Suding, K.N., 2010. Niche complementarity due to plasticity in resource use: plant partitioning of chemical N forms. Ecology 91, 3252–3260. https://doi.org/10.1890/09-1849.1.

Bale, N.J., Ding, S., Hopmans, E.C., Arts, M.G.I., Villanueva, L., Boschman, C., Haas, A.F., Schouten, S., Sinninghe Damsté, J.S., 2021. Lipidomics of environmental microbial communities. I: visualization of component distributions using untargeted analysis of high-resolution mass spectrometry data. Frontiers in Microbiology 12. https://doi.org/10.3389/fmicb.2021.659302.

Bates, D., Mächler, M., Bolker, B.M., Walker, S.C., 2015. Fitting linear mixed-effects models using lme4. Journal of Statistical Software 67, 1–48. https://doi.org/10.3389/fmicb.2021.659302.

Bentley, B.L., 1987. Nitrogen fixation by epiphylls in a tropical rainforest. Annals of the Missouri Botanical Garden 74, 234–241. https://doi.org/10.2307/2399396.

Bosak, T., Schubotz, F., de Santiago-Torio, A., Kuehl, J.V., Carlson, H.K., Watson, N., Daye, M., Summons, R.E., Arkin, A.P., Deutschbauer, A.M., 2016. System-wide adaptations of desulfovibrio alaskensis G20 to phosphate-limited conditions. PLoS One 11, e0168719. https://doi.org/10.1371/journal.pone.0168719.

Brand, W.A., Coplen, T., 2012. Stable isotope deltas: tiny, yet robust signatures in nature. Isotopes in Environmental and Health Studies 48, 393–409. https://doi.org/10.1080/10256016.2012.666977.

Brundish, D.E., Shaw, N., Baddiley, J., 1966. Bacterial glycolipids. Glycosyl diglycerides in gram-positive bacteria. Biochemical Journal 99, 546–549. https://doi.org/10.1042/bj0990546.

Butler, O.M., Manzoni, S., Warren, C.R., 2023. Community composition and physiological plasticity control microbial carbon storage across natural and experimental soil fertility gradients. ISME Journal 17, 2259–2269. https://doi.org/10.1038/s41396-023-01527-5.

Chambers, M.C., Maclean, B., Burke, R., Amodei, D., Ruderman, D.L., Neumann, S., Gatto, L., Fischer, B., Pratt, B., Egertson, J., Hoff, K., Kessner, D., Tasman, N., Shulman, N., Frewen, B., Baker, T.A., Brusniak, M.Y., Paulse, C., Creasy, D., Flashner, L., Kani, K., Moulding, C., Seymour, S.L., Nuwaysir, L.M., Lefebvre, B., Kuhlmann, F., Roark, J., Rainer, P., Detlev, S., Hemenway, T., Huhmer, A., Langridge, J., Connolly, B., Chadick, T., Holly, K., Eckels, J., Deutsch, E.W., Moritz, R.L., Katz, J.E., Agus, D.B., MacCoss, M., Tabb, D.L., Mallick, P., 2012. A cross-platform toolkit for mass spectrometry and proteomics. Nature Biotechnology 30, 918–920. https://doi.org/10.1038/nbt.2377.

Coskun, D., Britto, D.T., Shi, W., Kronzucker, H.J., 2017. How plant root exudates shape the nitrogen cycle. Trends in Plant Science 22, 661–673. https://doi.org/10.1016/j.tplants.2017.05.004.

Couvillion, S.P., Danczak, R.E., Naylor, D., Smith, M.L., Stratton, K.G., Paurus, V.L., Bloodsworth, K.J., Farris, Y., Schmidt, D.J., Richardson, R.E., Bramer, L.M., Fansler, S.J., Nakayasu, E.S., McDermott, J.E., Metz, T.O., Lipton, M.S., Jansson, J. K., Hofmockel, K.S., 2023. Rapid remodeling of the soil lipidome in response to a drying-rewetting event. Microbiome 11, 34. https://doi.org/10.1186/s40168-022-01427-4.

Dassen, S., Cortois, R., Martens, H., de Hollander, M., Kowalchuk, G.A., van der Putten, W.H., De Deyn, G.B., 2017. Differential responses of soil bacteria, fungi, archaea and protists to plant species richness and plant functional group identity. Molecular Ecology 26, 4085–4098. https://doi.org/10.1111/mec.14175.

de Bruijn, F.J., 2015. Biological nitrogen fixation. In: Lugtenberg, B. (Ed.), Principles of Plant-Microbe Interactions: Microbes for Sustainable Agriculture. Springer International Publishing, Cham, pp. 215–224. https://doi.org/10.1007/978-3-319-08575-3_23.

Degraeve-Guilbault, C., Brehelin, C., Haslam, R., Sayanova, O., Marie-Luce, G., Jouhet, J., Corellou, F., 2017. Glycerolipid characterization and nutrient deprivation-associated changes in the green picoalga ostreococcus tauri. Plant physiology 173, 2060–2080. https://doi.org/10.1104/pp.16.01467.

Ding, S., Bale, N.J., Hopmans, E.C., Villanueva, L., Arts, M.G.I., Schouten, S., Sinninghe Damsté, J.S., 2021. Lipidomics of environmental microbial communities. II: characterization using molecular networking and information theory. Frontiers in Microbiology 12, 659315. https://doi.org/10.3389/fmicb.2021.659315.

Ding, S., Lange, M., Lipp, J., Schwab, V.F., Chowdhury, S., Pollierer, M.M., Krause, K., Li, D.P., Kothe, E., Scheu, S., Welti, R., Hinrichs, K.U., Gleixner, G., 2020. Characteristics and origin of intact polar lipids in soil organic matter. Soil Biology and Biochemistry 151. https://doi.org/10.1016/j.soilbio.2020.108045.

Ding, S., von Meijenfeldt, F.A.B., Bale, N.J., Sinninghe Damsté, J.S., Villanueva, L., 2024. Production of structurally diverse sphingolipids by anaerobic marine bacteria in the euxinic Black Sea water column. The ISME Journal 18. https://doi.org/10.1093/ismejo/wrae153.

Du, E.Z., Terrer, C., Pellegrini, A.F.A., Ahlström, A., van Lissa, C.J., Zhao, X., Xia, N., Wu, X.H., Jackson, R.B., 2020. Global patterns of terrestrial nitrogen and phosphorus limitation. Nature Geoscience 13, 221. https://doi.org/10.1038/s41561-019-0530-4.

Dührkop, K., Fleischauer, M., Ludwig, M., Aksenov, A.A., Melnik, A.V., Meusel, M., Dorrestein, P.C., Rousu, J., Bocker, S., 2019. Sirius 4: a rapid tool for turning tandem mass spectra into metabolite structure information. Nature Methods 16, 299–302. https://doi.org/10.1038/s41592-019-0344-8.

Dührkop, K., Nothias, L.F., Fleischauer, M., Reher, R., Ludwig, M., Hoffmann, M.A., Petras, D., Gerwick, W.H., Rousu, J., Dorrestein, P.C., Bocker, S., 2021. Systematic classification of unknown metabolites using high-resolution fragmentation mass spectra. Nature Biotechnology 39, 462–471. https://doi.org/10.1038/s41587-020-0740-8.

Dynarski, K.A., Houlton, B.Z., 2018. Nutrient limitation of terrestrial free-living nitrogen fixation. New Phytologist 217, 1050–1061. https://doi.org/10.1111/nph.14905.

Eisenhauer, N., Lanoue, A., Strecker, T., Scheu, S., Steinauer, K., Thakur, M.P., Mommer, L., 2017. Root biomass and exudates link plant diversity with soil bacterial and fungal biomass. Scientific Reports 7, 44641. https://doi.org/10.1038/srep44641.

FAO, 1997. Unesco Soil Map of the World. Revised Legend with Corrections and Updates. World Soil Resources Report 60. FAO, Rome. Reprinted with updates as Technical paper 20. ISRIC, Wageningen. http://www.fao.org/fileadmin/user_upload/soils/docs/isricu_i9264_001.pdf. (Accessed 7 February 2025).

Gao, Y., Wang, H., Yang, F., Dai, X., Meng, S., Hu, M., Kou, L., Fu, X., 2023. Relationships among root exudation with root morphological and architectural traits vary with growing season. Tree Physiology 44. https://doi.org/10.1093/treephys/tpad118.
Geiger, O., Gonzalez-Silva, N., Lopez-Lara, I.M., Sohlenkamp, C., 2010. Amino acid-containing membrane lipids in bacteria. Progress in Lipid Research 49, 46–60. https://doi.org/10.1016/j.plipres.2009.08.002.
Gupta, V.V.S.R., Kroker, S.J., Hicks, M., Davoren, C.W., Descheemaeker, K., Llewellyn, R., 2014. Nitrogen cycling in summer active perennial grass systems in South Australia: non-symbiotic nitrogen fixation. Crop & Pasture Science 65, 1044–1056. https://doi.org/10.1071/Cp14109.
Gutschick, V.P., 1981. Evolved strategies in nitrogen acquisition by plants. The American Naturalist 118, 607–637. https://doi.org/10.1086/283858.
Hines, K.M., Waalkes, A., Penewit, K., Holmes, E.A., Salipante, S.J., Werth, B.J., Xu, L., 2017. Characterization of the mechanisms of daptomycin resistance among gram-positive bacterial pathogens by multidimensional lipidomics. mSphere 2. https://doi.org/10.1128/mSphere.00492-17.
Hoffmann, M.A., Nothias, L.-F., Ludwig, M., Fleischauer, M., Gentry, E.C., Witting, M., Dorrestein, P.C., Dührkop, K., Böcker, S., 2021. Assigning Confidence to Structural Annotations from Mass Spectra with COSMIC. bioRxiv. https://doi.org/10.1101/2021.03.18.435634.
Hütsch, B.W., Augustin, J., Merbach, W., 2002. Plant rhizodeposition - an important source for carbon turnover in soils. Journal of Plant Nutrition and Soil Science 165, 397–407. https://doi.org/10.1002/1522-2624(200208)165:4<397::AID-JPLN397>3.0.CO;2-C.
IAEA, 2009. Manual for the Use of Stable Isotopes in Entomology. International Atomic Energy Agency. https://www-pub.iaea.org/MTCD/Publications/PDF/IAEA_SI_web.pdf. (Accessed 7 February 2025).
Krapp, A., 2015. Plant nitrogen assimilation and its regulation: a complex puzzle with missing pieces. Current Opinion in Plant Biology 25, 115–122. https://doi.org/10.1016/j.pbi.2015.05.010.
Lange, M., Eisenhauer, N., Chen, H., Gleixner, G., 2023. Increased soil carbon storage through plant diversity strengthens with time and extends into the subsoil. Global Change Biology 29, 2627–2639. https://doi.org/10.1111/gcb.16641.
Lange, M., Eisenhauer, N., Sierra, C.A., Bessler, H., Engels, C., Griffiths, R.I., Mellado-Vazquez, P.G., Malik, A.A., Roy, J., Scheu, S., Steinbeiss, S., Thomson, B.C., Trumbore, S.E., Gleixner, G., 2015. Plant diversity increases soil microbial activity and soil carbon storage. Nature Communications 6, 6707. https://doi.org/10.1038/ncomms7707.
Lange, M., Koller-France, E., Hildebrandt, A., Oelmann, Y., Wilcke, W., Gleixner, G., 2019. How plant diversity impacts the coupled water, nutrient and carbon cycles. In: Eisenhauer, N., Bohan, D.A., Dumbrell, A.J. (Eds.), Mechanisms Underlying the Relationship between Biodiversity and Ecosystem Function. Academic Press, pp. 185–219. https://doi.org/10.1016/bs.aecr.2019.06.005.
Lange, M., Roth, V.N., Eisenhauer, N., Roscher, C., Dittmar, T., Fischer-Bedtke, C., Macé, O.G., Hildebrandt, A., Milcu, A., Mommer, L., Oram, N.J., Ravenek, J., Scheu, S., Schmid, B., Strecker, T., Wagg, C., Weigelt, A., Gleixner, G., 2021. Plant diversity enhances production and downward transport of biodegradable dissolved organic matter. Journal of Ecology 109, 1284–1297. https://doi.org/10.1111/1365-2745.13556.
Lassaletta, L., Billen, G., Grizzetti, B., Anglade, J., Garnier, J., 2014. 50 year trends in nitrogen use efficiency of world cropping systems: the relationship between yield and nitrogen input to cropland. Environmental Research Letters 9, 105011. https://doi.org/10.1088/1748-9326/9/10/105011.
Libohova, Z., Seybold, C., Wysocki, D., Wills, S., Schoeneberger, P., Williams, C., Lindbo, D., Stott, D., Owens, P.R., 2018. Reevaluating the effects of soil organic matter and other properties on available water-holding capacity using the National Cooperative Soil Survey Characterization Database. Journal of Soil and Water Conservation 73, 411–421. https://doi.org/10.2489/jswc.73.4.411.
Lu, T., Ke, M., Lavoie, M., Jin, Y., Fan, X., Zhang, Z., Fu, Z., Sun, L., Gillings, M., Penuelas, J., Qian, H., Zhu, Y.G., 2018. Rhizosphere microorganisms can influence the timing of plant flowering. Microbiome 6, 231. https://doi.org/10.1186/s40168-018-0615-0.
Mason-Jones, K., Breidenbach, A., Dyckmans, J., Banfield, C.C., Dippold, M.A., 2023. Intracellular carbon storage by microorganisms is an overlooked pathway of biomass growth. Nature Communications 14, 2240. https://doi.org/10.1038/s41467-023-37713-4.
Mason-Jones, K., Robinson, S.L., Veen, G.F.C., Manzoni, S., van der Putten, W.H., 2022. Microbial storage and its implications for soil ecology. The ISME Journal 16, 617–629. https://doi.org/10.1038/s41396-021-01110-w.
Meier, I.C., Finzi, A.C., Phillips, R.P., 2017. Root exudates increase N availability by stimulating microbial turnover of fast-cycling N pools. Soil Biology and Biochemistry 106, 119–128. https://doi.org/10.1016/j.soilbio.2016.12.004.
Meija, J., Coplen, T.B., Berglund, M., Brand, W.A., De Bièvre, P., Gröning, M., Holden, N. E., Irrgeher, J., Loss, R.D., Walczyk, T., Prohaska, T., 2016. Atomic weights of the elements 2013 (IUPAC technical report). Pure and Applied Chemistry 88, 265–291. https://doi.org/10.1515/pac-2015-0305.
Nothias, L.F., Petras, D., Schmid, R., Duhrkop, K., Rainer, J., Sarvepalli, A., Protsyuk, I., Ernst, M., Tsugawa, H., Fleischauer, M., Aicheler, F., Aksenov, A.A., Alka, O., Allard, P.M., Barsch, A., Cachet, X., Caraballo-Rodriguez, A.M., Da Silva, R.R., Dang, T., Garg, N., Gauglitz, J.M., Gurevich, A., Isaac, G., Jarmusch, A.K., Kamenik, Z., Kang, K.B., Kessler, N., Koester, I., Korf, A., Le Gouellec, A., Ludwig, M., Martin, H.C., McCall, L.I., McSayles, J., Meyer, S.W., Mohimani, H., Morsy, M., Moyne, O., Neumann, S., Neuweger, H., Nguyen, N.H., Nothias-Esposito, M., Paolini, J., Phelan, V.V., Pluskal, T., Quinn, R.A., Rogers, S., Shrestha, B., Tripathi, A., van der Hooft, J.J.J., Vargas, F., Weldon, K.C., Witting, M., Yang, H., Zhang, Z., Zubeil, F., Kohlbacher, O., Bocker, S., Alexandrov, T., Bandeira, N., Wang, M., Dorrestein, P.C., 2020. Feature-based molecular networking in the GNPS analysis environment. Nature Methods 17, 905–908. https://doi.org/10.1038/s41592-020-0933-6.
Oelmann, Y., Buchmann, N., Gleixner, G., Habekost, M., Roscher, C., Rosenkranz, S., Schulze, E.D., Steinbeiss, S., Temperton, V.M., Weigelt, A., Weisser, W.W., Wilcke, W., 2011. Plant diversity effects on aboveground and belowground N pools in temperate grassland ecosystems: development in the first 5 years after establishment. Global Biogeochemical Cycles 25. https://doi.org/10.1029/2010gb003869.
Oksanen, J., Simpson, G.L., Blanchet, F.G., Kindt, R., Legendre, P., Minchin, P.R., O'Hara, R.B., Solymos, P., Stevens, M.H.H., Szoecs, E., Wagner, H.. others, a., 2022. vegan, Community Ecology Package, R package. version 2.6-4. ed. https://CRAN.R-project.org/package=vegan. (Accessed 7 February 2025).
Phillips, R.P., Finzi, A.C., Bernhardt, E.S., 2011. Enhanced root exudation induces microbial feedbacks to N cycling in a pine forest under long-term CO2 fumigation. Ecology Letters 14, 187–194. https://doi.org/10.1111/j.1461-0248.2010.01570.x.
Pluskal, T., Castillo, S., Villar-Briones, A., Oresic, M., 2010. MZmine 2: modular framework for processing, visualizing, and analyzing mass spectrometry-based molecular profile data. BMC Bioinformatics 11, 395. https://doi.org/10.1186/1471-2105-11-395.
Poole, P., Ramachandran, V., Terpolilli, J., 2018. Rhizobia: from saprophytes to endosymbionts. Nature Reviews Microbiology 16, 291–303. https://doi.org/10.1038/nrmicro.2017.171.
Prommer, J., Walker, T.W.N., Wanek, W., Braun, J., Zezula, D., Hu, Y., Hofhansl, F., Richter, A., 2020. Increased microbial growth, biomass, and turnover drive soil organic carbon accumulation at higher plant diversity. Global Change Biology 26, 669–681. https://doi.org/10.1111/gcb.14777.
Ramette, A., 2007. Multivariate analyses in microbial ecology. FEMS Microbiology Ecology 62, 142–160. https://doi.org/10.1111/j.1574-6941.2007.00375.x.
Reed, S.C., Cleveland, C.C., Townsend, A.R., 2011. Functional ecology of free-living nitrogen fixation: a contemporary perspective. Annual Review of Ecology, Evolution, and Systematics 42, 489–512. https://doi.org/10.1146/annurev-ecolsys-102710-145034.
Richardson, K., Steffen, W., Lucht, W., Bendtsen, J., Cornell, S.E., Donges, J.F., Druke, M., Fetzer, I., Bala, G., von Bloh, W., Feulner, G., Fiedler, S., Gerten, D., Gleeson, T., Hofmann, M., Huiskamp, W., Kummu, M., Mohan, C., Nogues-Bravo, D., Petri, S., Porkka, M., Rahmstorf, S., Schaphoff, S., Thonicke, K., Tobian, A., Virkki, V., Wang-Erlandsson, L., Weber, L., Rockstrom, J., 2023. Earth beyond six of nine planetary boundaries. Science Advances 9. https://doi.org/10.1126/sciadv.adh2458.
Riekhof, W.R., Naik, S., Bertrand, H., Benning, C., Voelker, D.R., 2014. Phosphate starvation in fungi induces the replacement of phosphatidylcholine with the phosphorus-free betaine lipid diacylglyceryl-N,N,N-trimethylhomoserine. Eukaryotic Cell 13, 749–757. https://doi.org/10.1128/EC.00004-14.
Roscher, C., Schumacher, J., Baade, J., Wilcke, W., Gleixner, G., Weisser, W.W., Schmid, B., Schulze, E.D., 2004. The role of biodiversity for element cycling and trophic interactions: an experimental approach in a grassland community. Basic and Applied Ecology 5, 107–121. https://doi.org/10.1078/1439-1791-00216.
Rosner, B., 1983. Percentage points for a generalized esd many-outlier procedure. Technometrics 25, 165–172. https://doi.org/10.2307/1268549.
Scheibe, A., Spohn, M., 2022. N2 fixation per unit microbial biomass increases with aridity. Soil Biology and Biochemistry 172, 108733. https://doi.org/10.1016/j.soilbio.2022.108733.
Schmid, B., Baruffol, M., Wang, Z., Niklaus, P.A., 2017. A guide to analyzing biodiversity experiments. Journal of Plant Ecology 10, 91–110. https://doi.org/10.1093/jpe/rtw107.
Schrumpf, M., Schulze, E.D., Kaiser, K., Schumacher, J., 2011. How accurately can soil organic carbon stocks and stock changes be quantified by soil inventories? Biogeosciences 8, 1193–1212. https://doi.org/10.5194/bg-8-1193-2011.
Schubotz, F., 2019. Membrane homeostasis upon nutrient (C, N, P) limitation. In: Geiger, O. (Ed.), Biogenesis of Fatty Acids, Lipids and Membranes. Springer International Publishing, Cham, pp. 823–847. https://doi.org/10.1007/978-3-319-50430-8_59.
Schubotz, F., Wakeham, S.G., Lipp, J.S., Fredricks, H.F., Hinrichs, K.U., 2009. Detection of microbial biomass by intact polar membrane lipid analysis in the water column and surface sediments of the Black Sea. Environmental Microbiology 11, 2720–2734. https://doi.org/10.1111/j.1462-2920.2009.01999.x.
Scott, C.C., Finnerty, W.R., 1976. Characterization of intracytoplasmic hydrocarbon inclusions from the hydrocarbon-oxidizing Acinetobacter species HO1-N. Journal of Bacteriology 127, 481–489. https://doi.org/10.1128/jb.127.1.481-489.1976.
Semeniuk, A., Sohlenkamp, C., Duda, K., Holzl, G., 2014. A bifunctional glycosyltransferase from Agrobacterium tumefaciens synthesizes monoglucosyl and glucuronosyl diacylglycerol under phosphate deprivation. Journal of Biological Chemistry 289, 10104–10114. https://doi.org/10.1074/jbc.M113.519298.
Shannon, P., Markiel, A., Ozier, O., Baliga, N.S., Wang, J.T., Ramage, D., Amin, N., Schwikowski, B., Ideker, T., 2003. Cytoscape: a software environment for integrated models of biomolecular interaction networks. Genome Research 13, 2498–2504. https://doi.org/10.1101/gr.1239303.
Shen, X., Yang, F., Xiao, C.W., Zhou, Y., 2020. Increased contribution of root exudates to soil carbon input during grassland degradation. Soil Biology and Biochemistry 146. https://doi.org/10.1016/j.soilbio.2020.107817.
Smercina, D.N., Evans, S.E., Friesen, M.L., Tiemann, L.K., 2019a. Optimization of the 15N2 incorporation and acetylene reduction methods for free-living nitrogen fixation. Plant and Soil 445, 595–611. https://doi.org/10.1007/s11104-019-04307-3.

Smercina, D.N., Evans, S.E., Friesen, M.L., Tiemann, L.K., 2019b. To fix or not to fix: controls on free-living nitrogen fixation in the rhizosphere. Applied and Environmental Microbiology 85. https://doi.org/10.1128/AEM.02546-18.

Sohlenkamp, C., Geiger, O., 2016. Bacterial membrane lipids: diversity in structures and pathways. FEMS Microbiology Reviews 40, 133–159. https://doi.org/10.1093/femsre/fuv008.

Strobel, B.W., 2001. Influence of vegetation on low-molecular-weight carboxylic acids in soil solution - a review. Geoderma 99, 169–198. https://doi.org/10.1016/S0016-7061(00)00102-6.

Sturt, H.F., Summons, R.E., Smith, K., Elvert, M., Hinrichs, K.U., 2004. Intact polar membrane lipids in prokaryotes and sediments deciphered by high-performance liquid chromatography/electrospray ionization multistage mass spectrometry–new biomarkers for biogeochemistry and microbial ecology. Rapid Communications in Mass Spectrometry 18, 617–628. https://doi.org/10.1002/rcm.1378.

Tatituri, R.V., Brenner, M.B., Turk, J., Hsu, F.F., 2012. Structural elucidation of diglycosyl diacylglycerol and monoglycosyl diacylglycerol from Streptococcus pneumoniae by multiple-stage linear ion-trap mass spectrometry with electrospray ionization. Journal of Mass Spectrometry 47, 115–123. https://doi.org/10.1002/jms.2033.

Vences-Guzman, M.A., Geiger, O., Sohlenkamp, C., 2012. Ornithine lipids and their structural modifications: from A to E and beyond. FEMS Microbiology Letters 335, 1–10. https://doi.org/10.1111/j.1574-6968.2012.02623.x.

Wang, M., Carver, J.J., Phelan, V.V., Sanchez, L.M., Garg, N., Peng, Y., Nguyen, D.D., Watrous, J., Kapono, C.A., Luzzatto-Knaan, T., Porto, C., Bouslimani, A., Melnik, A. V., Meehan, M.J., Liu, W.T., Crusemann, M., Boudreau, P.D., Esquenazi, E., Sandoval-Calderon, M., Kersten, R.D., Pace, L.A., Quinn, R.A., Duncan, K.R., Hsu, C. C., Floros, D.J., Gavilan, R.G., Kleigrewe, K., Northen, T., Dutton, R.J., Parrot, D., Carlson, E.E., Aigle, B., Michelsen, C.F., Jelsbak, L., Sohlenkamp, C., Pevzner, P., Edlund, A., McLean, J., Piel, J., Murphy, B.T., Gerwick, L., Liaw, C.C., Yang, Y.L., Humpf, H.U., Maansson, M., Keyzers, R.A., Sims, A.C., Johnson, A.R., Sidebottom, A. M., Sedio, B.E., Klitgaard, A., Larson, C.B., P, C.A.B., Torres-Mendoza, D., Gonzalez, D.J., Silva, D.B., Marques, L.M., Demarque, D.P., Pociute, E., O'Neill, E.C., Briand, E., Helfrich, E.J.N., Granatosky, E.A., Glukhov, E., Ryffel, F., Houson, H., Mohimani, H., Kharbush, J.J., Zeng, Y., Vorholt, J.A., Kurita, K.L., Charusanti, P., McPhail, K.L., Nielsen, K.F., Vuong, L., Elfeki, M., Traxler, M.F., Engene, N., Koyama, N., Vining, O.B., Baric, R., Silva, R.R., Mascuch, S.J., Tomasi, S., Jenkins, S., Macherla, V., Hoffman, T., Agarwal, V., Williams, P.G., Dai, J., Neupane, R., Gurr, J., Rodriguez, A.M.C., Lamsa, A., Zhang, C., Dorrestein, K., Duggan, B.M., Almaliti, J., Allard, P.M., Phapale, P., Nothias, L.F., Alexandrov, T., Litaudon, M., Wolfender, J. L., Kyle, J.E., Metz, T.O., Peryea, T., Nguyen, D.T., VanLeer, D., Shinn, P., Jadhav, A., Muller, R., Waters, K.M., Shi, W., Liu, X., Zhang, L., Knight, R., Jensen, P.R., Palsson, B.O., Pogliano, K., Linington, R.G., Gutierrez, M., Lopes, N.P., Gerwick, W. H., Moore, B.S., Dorrestein, P.C., Bandeira, N., 2016. Sharing and community curation of mass spectrometry data with global natural products social molecular networking. Nature Biotechnology 34, 828–837. https://doi.org/10.1038/nbt.3597.

Warren, C.R., 2020. Soil microbial populations substitute phospholipids with betaine lipids in response to low P availability. Soil Biology and Biochemistry 140. https://doi.org/10.1016/j.soilbio.2019.107655.

Warren, C.R., Butler, O.M., 2024. Phosphorus drives adaptive shifts in membrane lipid pools and synthesis between soils. Soil Biology and Biochemistry 192. https://doi.org/10.1016/j.soilbio.2024.109387.

Weber, K., Burow, M., 2018. Nitrogen - essential macronutrient and signal controlling flowering time. Physiologia Plantarum 162, 251–260. https://doi.org/10.1111/ppl.12664.

Weigelt, A., Weisser, W.W., Buchmann, N., Scherer-Lorenzen, M., 2009. Biodiversity for multifunctional grasslands: equal productivity in high-diversity low-input and low-diversity high-input systems. Biogeosciences 6, 1695–1706. https://doi.org/10.5194/bg-6-1695-2009.

Weisser, W.W., Roscher, C., Meyer, S.T., Ebeling, A., Luo, G.J., Allan, E., Besser, H., Barnard, R.L., Buchmann, N., Buscot, F., Engels, C., Fischer, C., Fischer, M., Gessler, A., Gleixner, G., Halle, S., Hildebrandt, A., Hillebrand, H., de Kroon, H., Lange, M., Leimer, S., Le Roux, X., Milcu, A., Mommer, L., Niklaus, P.A., Oelmann, Y., Proulx, R., Roy, J., Scherber, C., Scherer-Lorenzen, M., Scheu, S., Tscharntke, T., Wachendorf, M., Wagg, C., Weigelt, A., Wilcke, W., Wirth, C., Schulze, E.D., Schmid, B., Eisenhauer, N., 2017. Biodiversity effects on ecosystem functioning in a 15-year grassland experiment: patterns, mechanisms, and open questions. Basic and Applied Ecology 23, 1–73. https://doi.org/10.1016/j.baae.2017.06.002.

White, D.C., Davis, W.M., Nickels, J.S., King, J.D., Bobbie, R.J., 1979. Determination of the sedimentary microbial biomass by extractible lipid phosphate. Oecologia 40, 51–62. https://doi.org/10.1007/BF00388810.

Wörmer, L., Lipp, J.S., Hinrichs, K.-U., 2015. Comprehensive analysis of microbial lipids in environmental samples through HPLC-MS protocols. In: McGenity, T.J., Timmis, K.N., Nogales, B. (Eds.), Hydrocarbon and Lipid Microbiology Protocols: Petroleum, Hydrocarbon and Lipid Analysis. Springer Berlin Heidelberg, Berlin, Heidelberg, pp. 289–317. https://doi.org/10.1007/8623_2015_183.

Wörmer, L., Lipp, J.S., Schröder, J.M., Hinrichs, K.-U., 2013. Application of two new LC–ESI–MS methods for improved detection of intact polar lipids (IPLs) in environmental samples. Organic Geochemistry 59, 10–21. https://doi.org/10.1016/j.orggeochem.2013.03.004.

Zacharias, S., Wessolek, G., 2007. Excluding organic matter content from pedotransfer predictors of soil water retention. Soil Science Society of America Journal 71, 43–50. https://doi.org/10.2136/sssaj2006.0098.

Zechmeister-Boltenstern, S., Keiblinger, K.M., Mooshammer, M., Penuelas, J., Richter, A., Sardans, J., Wanek, W., 2015. The application of ecological stoichiometry to plant-microbial-soil organic matter transformations. Ecological Monographs 85, 133–155. https://doi.org/10.1890/14-0777.1.

Zhang, T., He, W., Liang, Q., Zheng, F., Xiao, X., Zeng, Z., Zhou, J., Yao, W., Chen, H., Zhu, Y., Zhao, J., Zheng, Y., Zhang, C., 2023. Lipidomic diversity and proxy implications of archaea from cold seep sediments of the South China Sea. Frontiers in Microbiology 14. https://doi.org/10.3389/fmicb.2023.1241958.

Zheng, M., Chen, H., Li, D., Luo, Y., Mo, J., 2020. Substrate stoichiometry determines nitrogen fixation throughout succession in southern Chinese forests. Ecology Letters 23, 336–347. https://doi.org/10.1111/ele.13437.

Zheng, M., Xu, M., Li, D., Deng, Q., Mo, J., 2023. Negative responses of terrestrial nitrogen fixation to nitrogen addition weaken across increased soil organic carbon levels. Science of The Total Environment 877. https://doi.org/10.1016/j.scitotenv.2023.162965.

Zuur, A.F., Ieno, E.N., Walker, N.J., Saveliev, A.A., Smith, G.M., 2009. Mixed Effects Models and Extensions in Ecology with R. Springer, New York. https://doi.org/10.1007/978-0-387-87458-6.